Kinetics and Catalysis, Vol. 44, No. 3, 2003, pp. 401–407. Translated from Kinetika i Kataliz, Vol. 44, No. 3, 2003, pp. 436–442.

VI RUSSIAN CONFERENCE ON CATALYTIC REACTION MECHANISMS (Moscow, October 1–5, 2002)

In situ ^{1}H NMR Imaging Study of Propagation of Concentration Waves in an Autocatalytic Reaction in a Fixed Granular Bed

I. V. Koptyug[1], A. A. Lysova[1, 2, 3], V. N. Parmon[2], and R. Z. Sagdeev[1]

[1] *International Tomography Center, Siberian Division, Russian Academy of Sciences, Novosibirsk, Russia*

[2] *Boreskov Institute of Catalysis, Siberian Division, Russian Academy of Sciences, Novosibirsk, 630090 Russia*

[3] *Novosibirsk State University, Novosibirsk, 630090 Russia*

Received November 4, 2002

Abstract—The *in situ* ^{1}H NMR technique was used to study the propagation of chemical waves during the liquid-phase Belousov–Zhabotinsky (BZ) reaction in a model fixed bed of grains consisting of chemically inert glass beads or quartz sand. The propagation of autocatalytic chemical waves in this bed is determined by the size of pores between the grains. The rate of wave front propagation is independent of the size of the grains involved in this bed but is much lower than that in the bulk of the homogenous aqueous phase. This may be attributed to the difference in the effective diffusion coefficients in the homogeneous liquid phase and in the bed.

INTRODUCTION

An essential feature of many heterogeneous catalytic reactions is the involvement of nonlinear and autocatalytic stages. Therefore, the complex kinetic behavior of such reactions may involve reaction rate oscillations, chemical (concentration) waves at the catalyst surface, and periodic variations in the reactant and intermediate concentrations or in the temperature of the catalyst grain [1–5]. Until now, the propagation of the concentration waves for heterogeneous systems has only been studied at single crystalline surfaces. Conventional *in situ* methods can barely be used to investigate such phenomena in the catalyst bed, because these beds are three-dimensional and optically nontransparent. Taking this into account, NMR imaging seems to be rather promising in the study of spatially organized chemical processes in bulk beds.

In this work, we used NMR imaging to study the self-oscillating reaction in a fixed granular bed imitating the catalyst loading. We chose the liquid-phase rather than the heterogeneous Belousov–Zhabotinsky (BZ) reaction, for which the dynamics of wave front propagation was investigated in homogeneous media by NMR microimaging (MRM) [6, 7]. The advantage of MRM is that it allows one to perform *in situ* studies of chemical wave propagation in the course of the autocatalytic reaction, because this method does not affect the course of the reaction. Earlier [8–12], we employed NMR imaging to examine various physicochemical processes occurring in porous grains and beds consisting of porous grains [8–12]. In this work, we used it again to investigate the occurrence of autocatalytic chemical reactions in the granular bed.

EXPERIMENTAL

Experiments were carried out using a DRX 300 Avance NMR spectrometer (Bruker). The setup contained a superconducting magnet with a vertical bore to put the sample in and an imaging accessory capable of delivering gradient magnetic field pulses up to 100 G/cm. In the experiments, the ^{1}H NMR signal of liquid water was registered at a frequency of 299.13 MHz.

The initial concentrations of reactants in the reaction solution during the BZ reaction were as follows: H_2SO_4, 0.2 M; KBr, 0.06 M; H_3PO_4, 2.8 M; malonic acid, 0.15 M; and $NaBrO_3$, 0.05 M. $MnSO_4$ (0.0006 M) was used as a homogenous catalyst for the BZ reaction. In the experiments performed in the homogenous medium, the solution was stabilized by starch (0.7 wt %). A bed of glass beads with diameters of 0.5 and 3.2 mm and quartz sand with a particle size of 0.1 mm were used as a model porous matrix. In some experiments, the bromate concentration was varied from 0.04 to 0.10 M. All experiments were conducted at room temperature. Quartz sand or glass beads with a diameter of 0.5 mm were loaded into a glass ampule with a diameter of 5 mm, whereas beads with a diameter of 3.2 mm were put into an ampule with a diameter of 10 mm.

NMR imaging uses gradient magnetic field pulses, thus allowing one to obtain spatial information on the state of the object studied [13–16]. When a linear gradient of the magnetic field is applied in addition to a constant magnetic field, the resonance frequency becomes a function of the nuclear spin coordinate along the gradient, and the distribution of nuclear spins (the substance amount) in the sample along the chosen direction can be determined.

The perpendicular application of two or three magnetic field gradients makes it possible to obtain two- or

0023-1584/03/4403-0401$25.00

Conventional Field–Koros–Noyes mechanism for the BZ reaction for malonic acid oxidation [17]

Process **A**	
$3(Br^- + HOBr + H^+ \rightleftharpoons Br_2 + H_2O)$	(I)
$Br^- + HBrO_2 + H^+ \rightleftharpoons 2HOBr$	(II)
$Br^- + BrO_3^- + 2H^+ \rightleftharpoons HOBr + HBrO_2$	(III)
$5Br^- + BrO_3^- + 6H^+ \rightleftharpoons 3Br_2 + 3H_2O$	(A)
Process **B**	
$2HBrO_2 \rightleftharpoons HOBr + BrO_3^- + H^+$	(IV)
$2(HBrO_2 + BrO_3^- + H^+ \rightleftharpoons 2BrO_2^\bullet + H_2O)$	(V)
$4(BrO_2^\bullet + M^{n+} + H^+ \rightleftharpoons M^{(n+1)+} + HBrO_2)$	(VI)
$BrO_3^- + 4M^{n+} + 5H^+ \rightleftharpoons 4M^{(n+1)+} + HOBr + 2H_2O$	(B)
Process **C**	
$CH_2(COOH)_2 \rightleftharpoons (HO)_2C{=}CHCOOH$	(VII)
$(HO)_2C{=}CHCOOH + Br_2 \longrightarrow BrCH(COOH)_2 + H^+ + Br^-$	(VIII)
$2M^{(n+1)+} + CH_2(COOH)_2 + BrCH(COOH)_2 \longrightarrow fBr^- +$ other products	(IX)

Note: M^{n+} and $M^{(n+1)+}$ are the catalyst cations in different oxidation states; f is the adjustable stoichiometic parameter.

three-dimensional images of the sample with a spatial resolution of hundreds and thousands of microns.

RESULTS AND DISCUSSION

The BZ reaction comprises the oxidation of certain organic compounds (malonic and citric acids) by the bromate anion catalyzed by certain transition metal ions (Ce(III), Mn(II), and $Fe(phen)_3^{2+}$). The superposition of diffusion processes and nonlinear steps of this chemical reaction may lead to oscillations of the reactant and intermediate concentrations, as well as the formation of complex spatial–temporal wave structures at certain reactant concentrations. The commonly accepted mechanism of the BZ reaction is presented in the table. The overall oxidation of an organic substrate can be subdivided into three components: processes **A**, **B**, and **C**. The autocatalytic step of this scheme consists of reactions (V) and (VI) of process **B**, involving $HBrO_2$, which acts as an autocatalyst. It is important for NMR imaging that the oxidation state of the catalyst ion changes periodically in this process (see table), because the reduced (Mn^{2+}) and oxidized (Mn^{3+}) ions have different effects on the relaxation time of the protons of a solvent (water) when the manganese cations are used as a catalyst.

NMR imaging has been used to study the BZ reaction in homogenous media [6, 7], but it has not been used to study the effect of a heterogeneous medium on the system's behavior.

It is known that the spatial–wave structures formed in the BZ reaction are destroyed by the convective liquid flows. To prevent this destruction, one should either increase the viscosity of the reaction medium (for example, by introducing starch) or conduct the process in a heterogeneous matrix.

Preliminary experiments were performed in a homogeneous system. During the experiment, one-dimensional projections of the NMR signal intensity on the axis of the vertical ampule filled with the homogeneous reaction solution stabilized by starch were gradually registered every 3.2 s (Fig. 1). In the experiment, a change in the intensity of the NMR signal caused by the periodic variation in the oxidation state of the manganese ions in the course of the autocatalytic reaction (see table) was recorded. The paramagnetic cation Mn^{2+} shortens the relaxation time of water protons to a greater extent than the paramagnetic Mn^{3+} cation does, thus allowing one to obtain a T_1-contrast image by NMR imaging. The light gray color in Fig. 1 corresponds to the region of the more intensive NMR signal and, consequently, to the region of the less intensive NMR signal and, hence, to the region with the high Mn^{3+} concentration. The black color at the edges of the figure indicates the absence of the NMR signal in this region of the image (due to a decrease in the magnetic field intensity near the edges of a radio-frequency coil).

Figure 1 shows a synchronous change in the state of the reaction solution at the beginning of the process in the entire sample tube. Then the change in the oxidation state of the manganese cation caused by the chemical transformation starts to occur earlier in some parts of

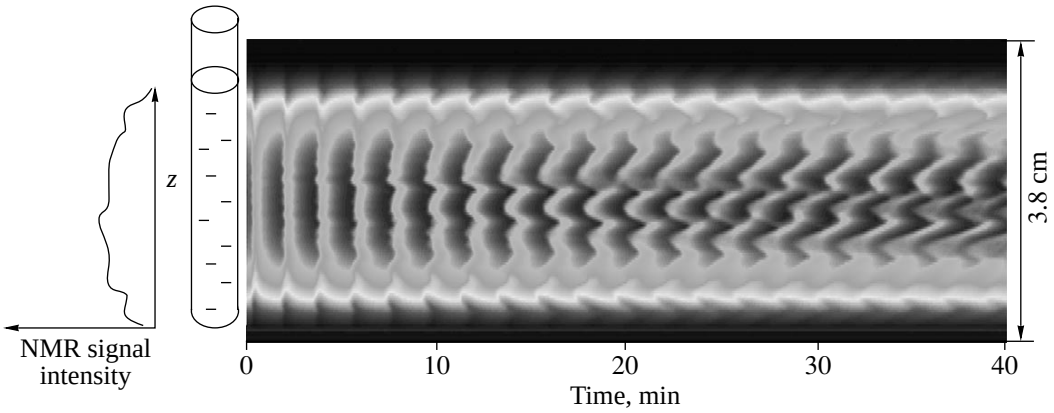

Fig. 1. Consecutive one-dimensional projections of the NMR signal intensity of the homogeneous reaction solution stabilized by starch in the ampule containing $[NaBrO_3]_0 = 0.05$ M. The spatial resolution is 320 μm and the detection time of each projection is 3.2 s.

the ampule, and the diffusion of reactants from these regions to the adjacent ones results in the propagation of the spherical concentration wave. The region behind the wave front remains in an unexcited state until diffusion allows the reactant concentration to attain values that are sufficient to repeat the autocatalytic reaction. Figure 1 presents the projection of each spherical wave, that is, two autocatalytic fronts propagating upwards and downwards from the point of wave generation.

Figure 2a shows how the BZ reaction occurs in a model grain layer consisting of chemically inert glass beads with a diameter of 0.5 mm. We obtained the consecutive two-dimensional projections of the NMR signal intensity onto the plane of the vertical axis of the ampule for the ampule filled with the reaction mixture and glass beads to the same level. In this experiment, the spherical wave source is located in the visible part of the ampule. This allowed us to directly observe how the wave propagated in the bed and how the spherical wave became planar when reaching the ampule wall. Figure 2a suggests that the spherical wave is generated with a certain frequency in the same point of the system. In our experiments, the rate of chemical wave propagation in the bed consisting of 0.5-mm beads was 1.5 ± 0.2 mm/min. The rate of wave propagation practically remains unchanged during the 90 min of the experiment, and the period of oscillations (i.e., the time between the instants of spherical wave generation) changes only slightly (Fig. 3a). Nevertheless, the oscillation period increases in the course of the experiment, apparently due to bromate consumption during the reaction.

Figure 4 shows a typical change in the intensity of the NMR signal during the reaction at an arbitrarily chosen location within the bed. This function is oscillating. The maxima correspond to the times when the manganese cation acting as the reaction catalyst is present mostly in the reduced Mn^{2+} state and the positions of minima correspond to the times when most of the catalyst is present in the oxidized state Mn^{3+}.

Figure 2b presents the consecutive two-dimensional images of the ampule with the reaction solution, which is also filled with 0.5-mm glass beads and with the homogeneous liquid layer covering the bed (i.e., when the level of the reaction solution is above the bed). In this experiment, the propagation of two wave fronts is observed: one is formed and propagates inside the bed and the other is formed in the solution and passes through the interface between the homogeneous phase and the bed, where it annihilates with the wave front propagating in the bed. In this case, wave propagation slows down by a factor of 2.7 when passing from the homogenous to the heterogeneous medium (the rate of wave propagation in the homogeneous aqueous medium is 4.4 ± 0.3 mm/min). Due to the effect of convective liquid flows, blurring of the wave front is observed when it propagates near the ampule walls where the bed porosity is higher than in the vest of the bed.

One possible reason for the rate change observed when the wave front enters the porous medium is the difference between the reactant concentrations in the granular bed (e.g., as a result of adsorption) and their bulk concentrations. Another reason is a decrease in the effective diffusion coefficient, which in the interstitial space of a porous medium is equal to $D \approx D_0 \frac{\varepsilon}{\tau}$ (D_0 is the molecular diffusivity, ε is the bed porosity, and τ is the tortuosity of thew porous space) [18]. Taking this into account, we conducted similar experiments with beds consisting of larger glass beads (3.2 mm). The rate of wave propagation in such beds remains practically unchanged and is equal to 1.8 ± 0.4 mm/min despite a nearly 40-fold change in the surface area. Therefore, the main reason behind rate variations observed when the wave enters the bed seems to be a change in the effective diffusion coefficient.

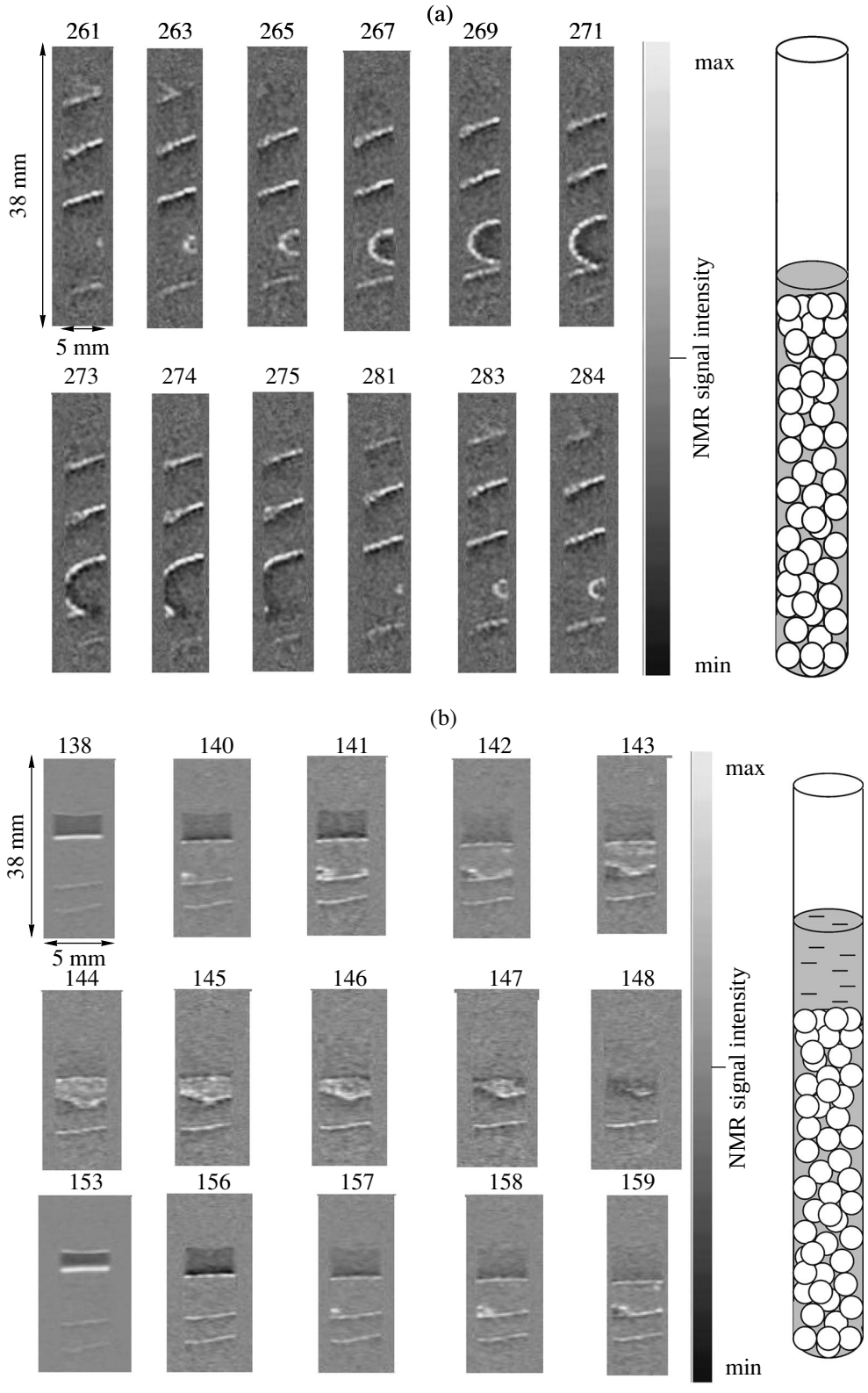

Fig. 2. Consecutive two-dimensional projections of the NMR-signal intensity in the vertical ampule with a diameter of 5 mm filled with 0.5-mm glass beads and the reaction solution with $[NaBrO_3]_0$ = (a, b) 0.05 and (c) 0.10 M in the plane of the vertical axis of the ampule. The level of the reaction solution in the ampule is (b) above or (a, c) equal to that of the bed. The spatial resolution is (320×230) μm^2, the detection time of each two-dimensional projection is 14.3 s, and the total time of the experiment is 122 min. The number of each image is given in the figure. To improve the contrast, each previous image was subtracted from the next one.

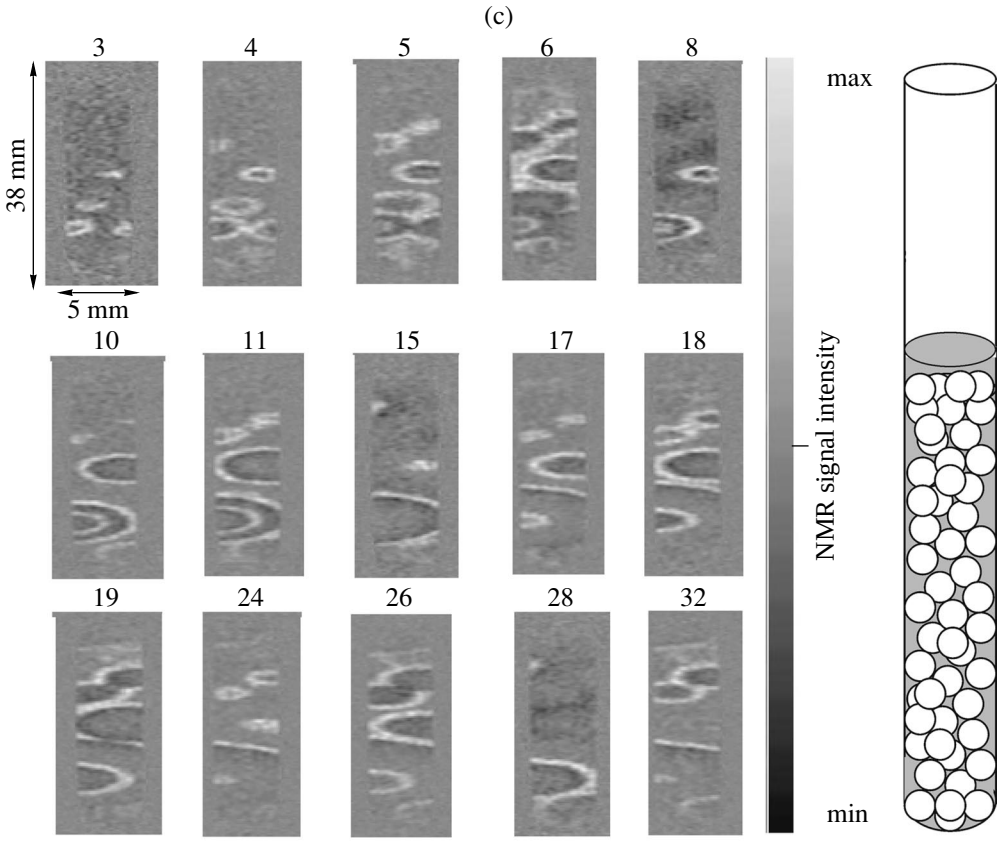

Fig. 2. (Contd.)

The fact that the chemical wave velocity remains unchanged on varying the size of the bed beads can easily be explained as follows. According to [19] the rate of the wave front in the reaction–diffusion system is $v \sim \sqrt{Dk}$, where D is the diffusion coefficient of the autocatalyst and k is the effective rate constant for the rate-limiting step of the overall process. For the bed consisting of spherical beads, the $\frac{\varepsilon}{\tau}$ ratio is practically independent of the size of the bed particles. Therefore, variations in the size of the porous matrix particles should not change the wave rate.

A twofold increase in the initial concentration of the bromate anions had a more pronounced effect than variations in the size of spherical particles in the bed. This caused a nearly twofold increase in the propagation velocity of the observed waves (the wave rate was 2.9 ± 0.5 mm/min at the initial $NaBrO_3$ concentration of 0.10 M). At the same time, the number of spherical wave sources increased drastically (Fig. 2c) and the period of oscillations decreased compared to the experiment with a lower bromate ion concentration (Fig. 3b). Figure 2c shows that the system initially behaved chaotically and then started to generate spherical waves after self-organization.

No wave effects were identified in the system with the cited reactant concentrations when a bed consisting of quartz sand (particle size, 0.1 mm) was used as a model porous medium. The absence of the wave activity of the system in this case can most likely be attributed to the existence of the critical radius of the wave front below which wave propagation is impossible. It is known that the rates of propagation of the spherical and planar waves are related by the equation $c_{sph} = c_{pl} + kD$, where k is the front curvature ($|k| = 1/r$, r is the spherical wave radius). Taking into account that $k < 0$ for the convex waves, the wave radius should be larger than the critical one to ensure successful wave generation $r_{cr} = \frac{D}{c_{pl}}$ [20]. For the velocities of propagation of planar waves typical of our systems equal to ~1.5 mm/min and the effective diffusion coefficient of small ions in the water phase of $\sim 2 \times 10^{-5}$ cm^2/s, the critical radius is of the order of 0.1 mm, thus precluding the observation of wave propagation in the bed consisting of quartz sand with nonspherical 0.1-mm particles. The pore sizes in the sand bed are smaller than their critical values for the given reaction conditions; therefore, when propagating in the system of connected pores, the chemical waves collapse when passing from the pores of smaller diameter to those of larger diameter.

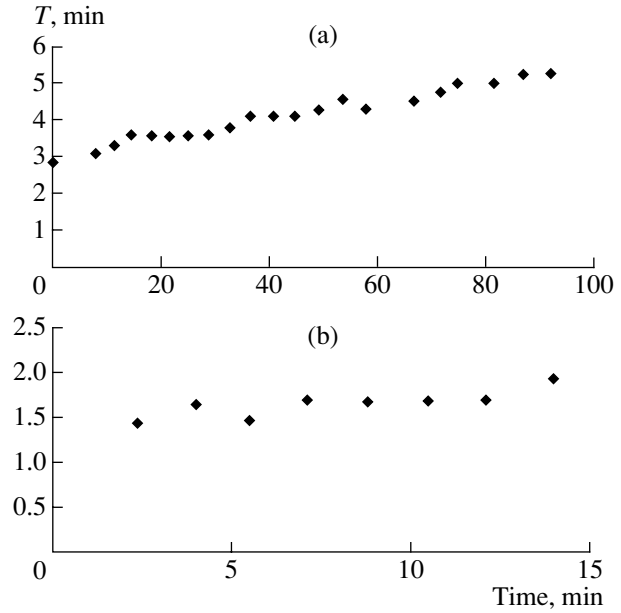

Fig. 3. Oscillation period (T) vs. time for the BZ reaction in the bed consisting of glass beads of diameter 0.5 mm. $[NaBrO_3]_0$ = (a) 0.05 and (b) 0.10 M.

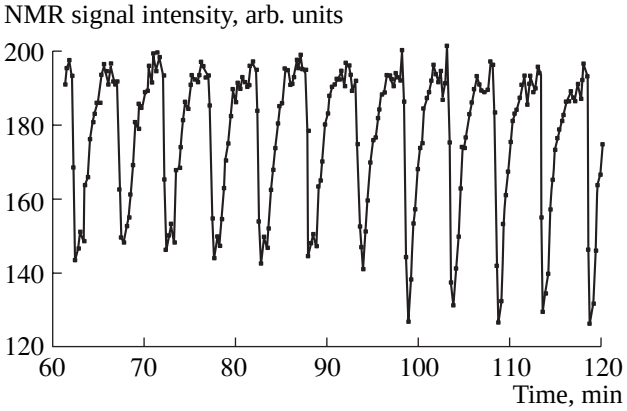

Fig. 4. Typical temporal dependence of the NMR signal intensity at an arbitrarily chosen location within the sample tube filled with the reaction solution and 0.5-mm glass beads. $[NaBrO_3]_0$ = 0.10 M.

Taking into account that the wave velocity increases with the bromate concentration, we tried to artificially enlarge the critical radius in the bed consisting of 0.5-mm glass beads by decreasing the bromate concentration. According to theoretical models, we should have observed the transformation of the wave regime into the one without waves (as in the case of sand). Indeed, the waves in the bed consisting of 0.5-mm glass beads disappeared even after an insignificant drop in the bromate anion concentration from 0.05 to 0.04 M because the critical radius became comparable with the pore size and the waves collapsed.

CONCLUSION

In this work, we used the autocatalytic Belousov–Zhabotinsky model reaction to demonstrate that NMR imaging can be used to detect and study the propagation of chemical waves in a model grain layer imitating the bed of catalyst grains. The transition from a homogeneous reaction medium to a heterogeneous one favors a decrease in the effect of the convective fluid flows on wave front propagation and allows the direct *in situ* observation of spherical and planar waves propagating in the bed. Moreover, the theoretically predicted retardation of chemical wave propagation compared to the homogenous phase is observed because the transition to the grain layer causes a decrease in the effective diffusion coefficient of the autocatalyst compared to the homogeneous liquid phase. The wave activity in the bed is observed only when the size of the pores between the bed grains is larger than a certain critical size determined by the rate of the propagation of the planar chemical wave, which is in qualitative agreement with the well-known theoretical models.

ACKNOWLEDGMENTS

This work was supported by the Russian Foundation for Basic Research (project nos. 02-03-32770, 03-03-06020), the “Leading Scientific Schools of Russia” program (project nos. 00-15-97446, 00-15-97450), the RAS commission on work with the young (competition-expert project no. 6 (1999)), and the Siberian Division of the Russian Academy of Sciences (integration project no. 41). A.A. Lysova also thanks the Zamaraev International Charitable Scientific Foundation.

REFERENCES

1. Imbihl, R. and Ertl, G., *Chem. Rev.*, 1995, vol. 95, p. 697.
2. Boreskov, G.K., *Geterogennyi kataliz* (Heterogeneous Catalysis), Moscow: Nauka, 1988.
3. Bazhin, N.M., Ivanchenko, V.I., and Parmon, V.N., *Termodinamika dlya khimikov* (Thermodynamics for Chemists), 2000, Moscow: Khimiya.
4. Khrustova, N., Michailov, A.S., and Imbihl, R., *J. Phys. Chem.*, 1997, vol. 107, p. 2096.
5. Slin’ko, M.M., Ukharskii, A.A., Reskov, N.V., and Jaeger, N.I., *Catal. Today*, 2001, vol. 70, p. 341.
6. Gao, Y., Cross, A.R., Amstrong, R.L., *J. Phys. Chem.*, 1996, vol. 100, p. 10159.
7. Tzalmona, A., Amstrong, R.L., Menzinger, M., Cross, A., and Lemaire, C., *Chem. Phys. Lett.*, 1990, vol. 174, p. 199.
8. Koptyug, I.V., Fenelonov, V.B., Khitrina, L.Yu., Sagdeev, R.Z., and Parmon, V.N., *J. Phys. Chem.*, 1998, vol. 102, p. 3090.
9. Koptyug, I.V., Kabanikhin, S.I., Iskakov, K.T., Fenelonov, V.B., Khitrina, L.Yu., Sagdeev, R.Z., and Parmon, V.N., *Chem. Eng. Sci.*, 2000, vol. 55, p. 1559.
10. *Sovremennye podkhody k issledovaniyu i opisaniyu protsessov sushki poristykh tel* (Modern Approaches to the

Study and Description of Processes of Drying of Porous Bodies), Parmon, V.N., Ed., Novosibirsk: Ross. Akad. Nauk, 2001, p. 300.

11. Koptyug, I.V., Kulikov, A.V., Lysova, A.A., Kirillov, V.A., Parmon, V.N., and Sagdeev, R.Z., *J. Am. Chem. Soc.*, 2002, vol. 124, p. 9684.
12. Koptyug, I.V., Kulikov, A.V., Lysova, A.A., Kirillov, V.A., Sagdeev, R.Z., and Parmon, V.N., *Dokl. Akad. Nauk*, 2002, vol. 385, no. 2, p. 205.
13. Kuhn, W., *Angew. Chem., Int. Ed. Engl.*, 1990, vol. 29, p. 1.
14. Talagala, S.L. and Lowe, I.J., *Concepts Magn. Reson.*, 1991, vol. 3, p. 145.
15. Koptyug, I.V. and Sagdeev, R.Z., *Usp. Khim.*, 2002, vol. 71, no. 7, p. 672.
16. Koptyug, I.V. and Sagdeev, R.Z., *Usp. Khim.*, 2002, vol. 71, no. 10, p. 899.
17. Field, R. and Burger, M., *Oscillations and Traveling Waves in Chemical Systems*, New York: Wiley, 1983.
18. Aerov, M.A., Todes, O.M., and Narinskii, D.A., *Apparaty so statsionarnym zernistym sloem* (Apparatus with Fixed Granular Layer), Leningrad: Khimiya, 1979.
19. Kuhnert, L., Krug, H.J., and Pohlmann, L., *J. Phys. Chem.*, 1985, vol. 89, p. 2022.
20. Toth, A., Gaspar, V., and Showalter, K., *J. Phys. Chem.*, 1994, vol. 98, p. 522.